CHEMISTRY OF
MATERIALS
Article

Chem. Mater. **2010,** *22,* 5823–5830 5823
DOI:10.1021/cm1018025

Photochemical Reactivity of Titania Films on $BaTiO_3$ Substrates: Origin of Spatial Selectivity

Nina V. Burbure, Paul A. Salvador, and Gregory S. Rohrer*

Department of Materials Science and Engineering, Carnegie Mellon University, Pittsburgh Pennsylvania, USA

Received June 28, 2010. Revised Manuscript Received September 10, 2010

Titania films, 15−100 nm thick, have been grown on $BaTiO_3$ substrates and used to photochemically reduce Ag^+ to Ag^0 and oxidize Pb^{2+} to Pb^{4+} under ultraviolet illumination. Atomic force microscopy was used to show that the reactions are spatially selective and that the pattern of products on the film surface reproduces the pattern of products on the bare substrate. The influence of the substrate on the pattern of reactants is diminished as the film thickness increases and is quenched when the film is donor-doped with Nb. The results indicate that for thin (15 nm) films, dipolar fields from the ferroelectric domains cause carriers generated in the substrate to travel through the film to react on the surface.

1. Introduction

Extensive studies of the photochemical reactivity of titania surfaces have been motivated by the possibility of catalyzing the photolysis of water.[1,2] However, when platinized titania powders are used as the catalyst, the recombination of photogenerated charge carriers and the back reaction of oxidized and reduced intermediates leads to low efficiency.[3,4] Ferroelectric materials have internal dipolar fields that separate photogenerated carriers,[5−7] and this has motivated several investigations of the photochemical properties of ferroelectrics.[8−12] It has been shown that the distribution of photochemically generated reaction products on ferroelectric surfaces is spatially localized, indicating that electrons and holes are spatially separated in the bulk.[13−19]

If the charge separating characteristics of the ferroelectric could be combined with the photocatalytic properties of titania, it might be possible to increase photolysis efficiency. Studies of powdered ferroelectric/titania composites motivated by this concept have shown some promising results.[20,21] Thin film heterostructures, investigated by Inoue,[22−24] have also been used to demonstrate that some benefits arise from the ferroelectric substrate. However, one characteristic of Inoue's structures was that the ferroelectrics were poled, which biases the heterostructure toward either the reduction or oxidation half reaction. In this case, it is possible that the complementary reaction, not favored by the poling, will limit the overall reaction rate.

More recently, Burbure et al.[25] reported on the photochemical reactivity of titania films supported by an unpoled, polycrystalline ferroelectric $BaTiO_3$ substrates. The differentiating characteristic of using unpoled substrates is that both halves of the redox process can be promoted on the same surface, while the two reactions are still spatially separated over distances large compared to diffusion lengths. Burbure et al.[25] showed that photochemically reduced Ag forms on the titania surface in patterns that are characteristic of the substrate's underlying domain structure. From this, it was surmised that the dipolar fields from the substrate separate charge carriers and reaction products on the film surface. Since that time, the phase and orientation relationships for the titania films on $BaTiO_3$ have been measured.[26] This has

---

*To whom correspondence should be addressed. E-mail: rohrer@cmu.edu.

(1) Fujishima, A.; Honda, K. *Nature* **1972**, *238*, 37.
(2) Linsebigler, A. L.; Lu, G.; Yates, J. T., Jr. *Chem. Rev.* **1995**, *95*, 735.
(3) Kudo, A.; Miseki, Y. *Chem. Soc. Rev.* **2009**, *38*, 253.
(4) Domen, K. In *Surface Photochemistry*; J. Wiley & Sons: Chichester, U.K., 1996; p 1.
(5) Brody, P. S. *Solid State Commun.* **1973**, *12*, 673.
(6) Brody, P. S. *J. Solid State Chem.* **1975**, *12*, 193.
(7) Fridkin, V. M. *Ferroelectrics* **1984**, *53*, 169.
(8) van Damme, H.; Hall, W. K. *J. Catal.* **1981**, *69*, 371.
(9) Inoue, Y.; Yoshioka, I.; Sato, K. *J. Phys. Chem.* **1984**, *88*, 1148.
(10) Inoue, Y.; Sato, K.; Sato, K.; Miyama, H. *J. Phys. Chem.* **1986**, *90*, 2809.
(11) Inoue, Y.; Hayashi, O.; Sato, K.; Kubokawa, T. *Proceedings of the 9th International Congress on Catalysis*, Calgary, Canada; Chemical Institute of Canada: Ottawa, Ontario, Canada, 1988; pp 1497−1504.
(12) Inoue, Y.; Hayashi, O.; Sato, K. *J. Chem. Soc., Faraday Trans.* **1990**, *86*, 2277.
(13) Inoue, Y. *Energy Environ. Sci.* **2009**, *2*, 364.
(14) Giocondi, J. L.; Rohrer, G. S. *Chem. Mater.* **2001**, *13*, 241.
(15) Giocondi, J. L.; Rohrer, G. S. *J. Phys. Chem. B* **2001**, *105*, 8275.
(16) Kalinin, S. V.; Bonnell, D. A.; Alvarez, T.; Lei, X.; Hu, Z.; Ferris, J. H.; Zhang, Q.; Dunn, S. *Nano Lett.* **2002**, *2*, 589.
(17) Hanson, J. N.; Rodriguez, B. J.; Nemanich, R. J.; Gruverman, A. *Nanotechnology* **2006**, *17*, 4946.
(18) Dunn, S.; Jones, P. M.; Gallardo, D. E. *J. Am. Chem. Soc.* **2007**, *129*, 8724.
(19) Giocondi, J. L.; Rohrer, G. S. *Top. Catal.* **2008**, *49*, 18.
(20) Li, S.; Lin, Y.-H.; Zhang, B.-P.; Li, J.-F.; Nan, C.-W. *J. Appl. Phys.* **2009**, *105*, 054310.
(21) Yeredla, R. R.; Xu, H. *J. Phys. Chem. C* **2008**, *112*, 532.
(22) Inoue, Y.; Sato, K.; Suzuki, S. *J. Phys. Chem.* **1985**, *89*, 2827.
(23) Inoue, Y.; Okamura, M.; Sato, K. *J. Phys. Chem.* **1985**, *89*, 5184.
(24) Inoue, Y.; Sato, K.; Sato, K.; Miyama, H. *Chem. Phys. Lett.* **1986**, *129*, 79.
(25) Burbure, N. V.; Salvador, P. A.; Rohrer, G. S. *J. Am. Ceram. Soc.* **2006**, *89*, 2943.
(26) Burbure, N. V.; Salvador, P. A.; Rohrer, G. S. *J. Am. Ceram. Soc.* **2010**, *93*, 2530.

enabled more detailed studies of the mechanism of the spatially selective reactivity and how it varies with the phase of titania, the surface orientation, and the film thickness. These results are reported here and in a companion paper.[27] In the companion paper,[27] the influence of titania phase and orientation on the reactivity of $TiO_2 \| BaTiO_3$ heterostructures is described. The purpose of this paper is to describe the mechanism of the spatially selective reactivity and how it varies with thickness. Using supported titania films with known structures, comparisons of the photochemical reduction of Ag^+ to Ag^0 and the oxidation of Pb^{2+} to Pb^{4+} indicate that reduction and oxidation occur on complementary areas of the film. Furthermore, the pattern of products on the surface exactly mimics that pattern on the bare substrate, suggesting that carriers from the substrate pass through the film and react on the surface.

2. Experimental Section

$BaTiO_3$ powder (Alfa Aesar, 99.7%) was ground and uniaxially compressed at 230 MPa to form cylinders with 11 mm diameters and 2−5 mm thicknesses. The samples were sintered in an alumina crucible containing excess $BaTiO_3$ powder to provide a barrier and minimize contamination from the crucible. The substrates were degassed for 10 h at 900 °C, sintered for 10 h at 1230 °C, and further annealed at 1360 °C to yield a dense polycrystal with approximately 50 μm diameter grains. A larger TiO_2 target was similarly prepared, but with a final anneal of 1600 °C for 24 h. To prepare the substrates for film growth, the samples were lapped flat using a 9 μm Al_2O_3 aqueous solution (Buehler), polished with a 0.02 μm colloidal silica solution (Logitech pm5 autopolisher), and thermally etched in air for 4 h at 1200 °C.

To estimate the material removal rate, the thickness of a $BaTiO_3$ substrate was periodically measured during the final polishing step using 0.02 μm colloidal silica. Based on these measurements, material was removed at 20 nm/sec. This value was used to estimate polishing times needed to remove films.

Titania films were grown using a Neocera PLD system with a KrF laser (λ = 248 nm) operating at a frequency of 3 Hz and at an energy density of 2 J/cm^2. The distance between the target and the substrate was 6 cm. A base pressure of 1.3×10^{-4} Pa was established before heating. Films were deposited at 700 °C in a dynamic vacuum of 1.3 Pa O_2. The films were cooled to room temperature in a static O_2 pressure of 670 Pa. Film thicknesses, determined by X-ray reflectivity measurements of films grown on $SrTiO_3$ single crystals placed next to select samples during growth, ranged from 10 to 110 nm.

To produce doped films, a second target was prepared by dissolving Nb_2O_5 in TiO_2. The Nb_2O_5 introduces *n*-type conductivity in accordance with the following equation:[28]

$$Nb_2O_5 \xrightarrow{TiO_2} 2Nb^{\bullet}_{Ti} + 2O^{*}_{O} + 2e' + \frac{1}{2}O_2(g) \qquad (1)$$

where $Nb^{\bullet}_{Ti}$ represents a substitutional Nb ion on a Ti site, O^{*}_{O} is an oxygen ion on an oxygen site and e′ is an electron in the conduction band. Assuming the films had the same composition as the target and that all of the donors were ionized, the carrier concentration in the doped films is estimated to be 3×10^{20}/cm^3, which is expected to exceed the intrinsic carrier concentration.[29]

X-ray diffraction indicated that the TiO_2 films deposited on polycrystalline $BaTiO_3$ contained both rutile and anatase. On a grain-by-grain basis, the crystallographic orientations of the substrate grains and the supported films were determined by electron backscatter diffraction. By comparing the results, orientation relationships for the substrate orientation and the film phase and orientation were determined. The procedure and results of this comparison have already been described.[26] The key results for the present study are that $BaTiO_3$ grains oriented near (100) support anatase films with the (001) orientation. $BaTiO_3$ grains with surface normals more than 26° from (100) support rutile films with a variety of orientations. These data were used to select grains with specific orientations for the studies of photochemical reactivity described here.

$AgNO_3$ (Fisher Scientific) was dissolved in deionized water to make a 0.115 M aqueous solution. Similarly, $Pb(C_2H_3O_2)_2$ (Fisher Scientific) was dissolved in deionized water to make a 0.0115 M solution. An O-ring on the sample surface was filled with the Ag or Pb bearing solution and illuminated by a 300 W Hg lamp. For the Pb oxidation reaction, it is known that Pb^{2+} is oxidized to Pb^{4+} and insoluble PbO_2 is deposited.[30,31] For the reduction of Ag^+ to Ag, it is known that silver deposits at the site of the reaction.[32,33] Energy dispersive spectroscopy in the scanning electron microscope has been used to confirm that the deposits produced in our experiments contain silver and lead. In general, the films were less reactive than the bare substrates. For the reduction of silver, the substrates were exposed for 3 s and the films for 15 s to create a comparable amount of reaction product. For the lead oxidation, the substrates were exposed for 180 s and the films were exposed for 270 s.

After exposure to light, the sample was washed in water, dried in air, and imaged by atomic force microscopy (AFM). Topographic AFM images were obtained in noncontact mode using a Veeco Digital Instruments Dimension 3100 AFM or a Veeco Digital Instruments CP-II. Representative regions were imaged before and after the reactions.

3. Results

The AFM images in Figure 1 compare the same area of the surface of a 15 nm thick film before reaction (a), after reaction in aqueous silver nitrate (c), and aqueous lead acetate solutions (e). In Figure 1a, some contrast results from features associated with the $BaTiO_3$ polycrystalline substrate microstructure; for example, three grain boundaries meet at a triple junction (TJ) and surface steps (S) form geometric patterns on some of the grains. The orientations of the three grains were not determined. Finally, there are also occasional pores and polishing scratches. Of more importance, there is noticeable "striped" contrast resulting from apparent 90° domain boundaries (D). There are two possible sources of this domain contrast. Some contrast results from topography created by differential polishing before film growth. Because the sample is

---

(27) Burbure, N. V.; Salvador, P. A.; Rohrer, G. S. *Chem. Mater* DOI: 10.1021/cm1018019.

(28) Bak, T.; Nowotny, J.; Rekas, M.; Sorrell, C. C. *J. Phys. Chem. Solids* **2003**, *64*, 1043.

(29) Breckenridge, R. G.; Hosler, W. R. *Phys. Rev.* **1953**, *91*, 793.

(30) Tanaka, K.; Harada, K.; Murata, S. *Solar Energy* **1986**, *36*, 159.

(31) Torres, J.; Cervera-March, S. *Chem. Eng. Sci.* **1992**, *47*, 3857.

(32) Clark, W. C.; Vondjidis, A. G. *J. Catal.* **1965**, *4*, 691.

(33) Herrmann, J.-M.; Disdier, J.; Pichat, P. *J. Catal.* **1988**, *113*, 72.

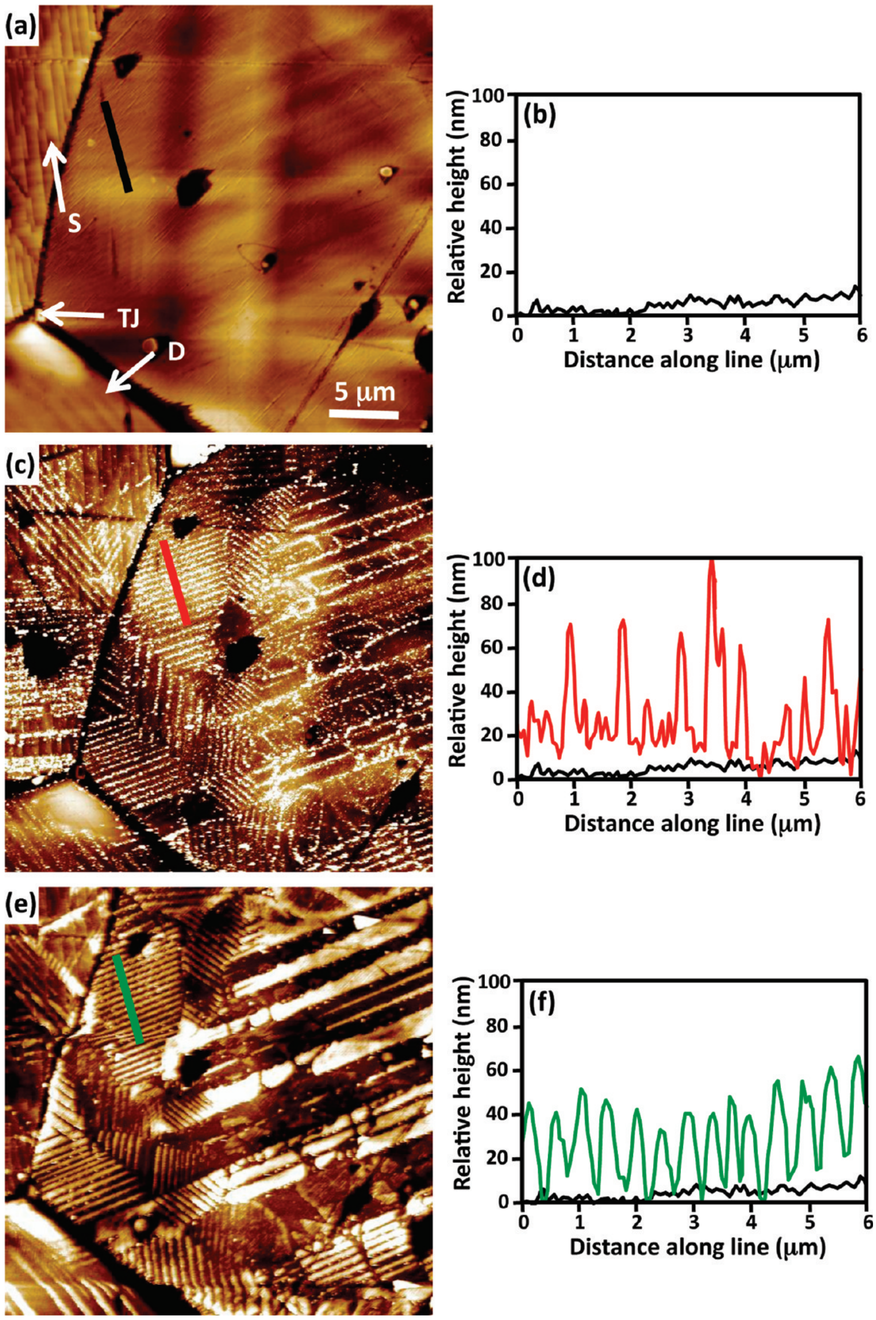

Figure 1. Topographic AFM images of a 15 nm thick TiO_2 film surface (a) before reaction, (c) after reaction with silver nitrate solution, and (e) after reaction in lead acetate solution. Contrast associated with steps (S), domains (D), and a grain boundary triple junction (TJ) are indicated by arrows. The black-to-white contrast in a, c, and e are 70, 55, and 80 nm, respectively. Panels b, d, and f compare the topography along the 6 μm traces indicated by the black, red, and green lines.

heated above the Curie temperature for film growth, these domains are removed, but the polishing induced topography remains. After deposition, the sample is cooled and new domains form that may also create surface relief. Hence, while some of the contrast is indicative of existing domain structure, some is purely historical and will not correlate with domains. The height profile along the black line in the image is plotted in Figure 1b.

An image of the same area of the surface after the silver reaction is shown in Figure 1c. The topography is now dominated by contrast from silver deposits. This is illustrated by Figure 1d, which compares the topography before and after the reaction along similar 6 μm traces shown by the black line in 1a and the red line in 1c, respectively. The silver deposits form in patterns that are characteristic of the $BaTiO_3$ domain structure and, in some cases, correlates with pre-existing contrast in Figure 1a. By wiping the surface clean with a tissue and sonicating in water and acetone, we removed the silver so that AFM images appeared the same as before the reaction. The sample was then exposed to UV light in a Pb-bearing solution, and the same area of the surface was imaged (see Figure 1e). In this case, the topographic contrast is now dominated by the lead containing deposits; Figure 1f compares the topography before and after the reaction along similar 6 μm traces shown by the black

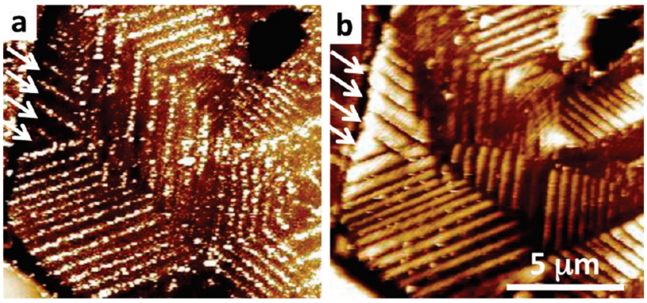

Figure 2. Topographic AFM images of a 15 nm thick TiO_2 film surface (a) after reaction with silver nitrate solution and (b) after reaction in lead acetate solution. These images are enlarged insets from Figure 1c and d. The arrows in the upper left corner draw attention to the complementary width of the reduced silver and oxidized lead stripes.

line in 1a and the green line in 1e, respectively. Again, the reaction product deposits in patterns consistent with the $BaTiO_3$ domain structure.

By comparing the contrast in Figure 1c and e, we can conclude that the lead containing and silver containing deposits form in different, complementary locations. This is highlighted by Figure 2, which shows enlarged subsets of Figures 1c and 1d from the regions to the immediate right of the triple junction. In sets of parallel domains where the Ag reduces on thin domains with wide gaps between them, the lead is oxidized on the wide domains with thin gaps between. To facilitate this comparison, four parallel white arrows point to regions that are relatively unreactive in Figure 2a and the same regions that are reactive in Figure 2b. The complementary patterns of deposits formed on these 15 nm thick titania films are analogous to the patterns observed on the bare $BaTiO_3$ surface.[15] The region in Figure 2 was selected because the clear difference in the thicknesses of the reactive and unreactive domains simplifies the comparison. However this is not always the case, and in some cases, the reducing domains are wider than the oxidizing domains (for example, see the lower left parts of the images in Figure 1). Finally, it should be recognized that the reactivity is not simply "on" or "off". Instead, the reactivity of the films are enhanced or suppressed to differing degrees in different areas, as can be seen in Figure 2.

A previous study of the $BaTiO_3$ substrate showed that the potential measured on the surface by scanning potential microscopy correlated exactly with the patterns of silver and lead deposition.[34] However, extensive scanning potential imaging of the titania film surface never revealed patterns that could be correlated with the domain structure of the substrate. This null observation suggests that the 15 nm thick titania film screens the polarization from $BaTiO_3$.

To determine how the positions of the reaction product on the film correlate to the domains in the substrate, the reactivity of the film was compared to the reactivity of the substrate after the film was removed by polishing. The image in Figure 3a shows the surface of a 15 nm thick film after a lead oxidation reaction. The white contrast corresponds to lead oxide. The film was then removed by polishing for 30 s. On the basis of our measured material removal rate (20 nm/s), the amount of material removed is approximately 40 times the film thickness. Although the removal rate was measured on the substrate rather than the film, it does not seem likely that the film is 40 times more wear resistant than the substrate and we can be confident that the film was removed.

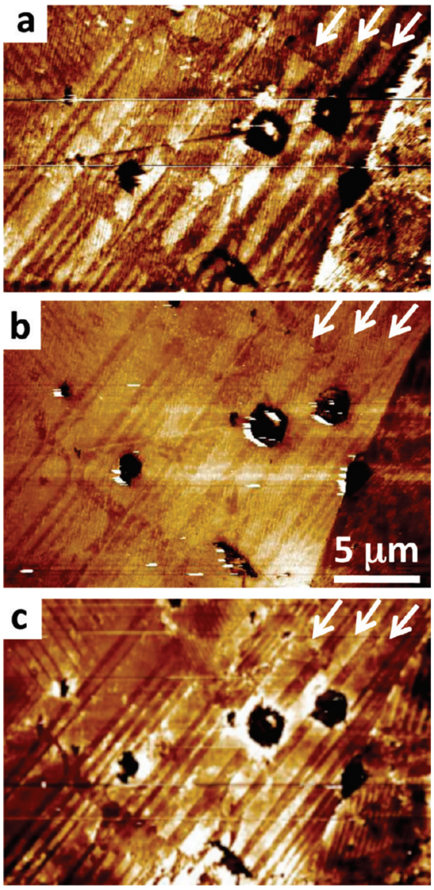

Figure 3. Topographic AFM images of (a) a 15 nm thick TiO_2 film surface after reaction in lead acetate solution, (b) the same location after removing the film by polishing, and (c) the same location after polishing and photochemically reacting with lead acetate solution. Black-to-white contrast is 50, 30, and 40 nm, respectively.

An AFM image of the same area after film removal is shown in Figure 3b. There is some contrast in the image that arises from differential removal rates of material in different domains (an observation that confirms that the entire titania film has been removed). The image in Figure 3c shows the same area of the $BaTiO_3$ surface after the photochemical oxidation of lead. Using the pores (black spots) in the image as fiducial marks, it is clear that the lead oxide deposits on the substrate are in the same positions as they were on the film. Three arrows have been added to the images to guide the eye. Considering the similarities of patterns of lead oxide in the images in Figures 3a and c, the spatially selective reactivity of the thin titania film is the same as the supporting $BaTiO_3$ substrate. This result is summarized by the schematic in Figure 4. Note that the geometry in this schematic assumes that the edges of the rectangular parallelepiped are orientated parallel to the pseudocubic

---

(34) Bhardwaj, A.; Burbure, N. V.; Gamalski, A.; Rohrer, G. S. *Chem. Mater.* **2010**, *22*, 3527.

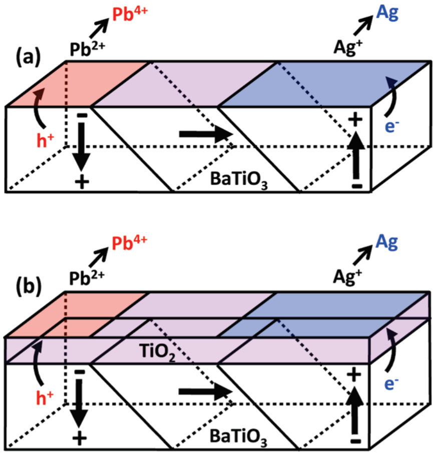

Figure 4. A schematic illustrating that domains in the substrate promote the same half reactions on both the bare substrate (a) and film (b) surfaces.

axes. Furthermore, the entire surface of the titania film can be reactive for oxidation or reduction, including the neutral domains. However, each reaction is promoted in some domains, suppressed in others, and has intermediate values in neutral domains. For heterostructures not perfectly oriented, the reactivity is expected to vary with the component of the polarization normal to the surface.

Photochemical reactions were also carried out on the films with different thicknesses. This is similar to an experiment reported earlier using grains of undetermined orientations.[25] In the present case, we selected only substrate grains within 5° of the (100) orientation. On the basis of previously published work, we know that these grains support anatase films with the [001] orientation.[26] Images of the film surfaces after the photochemical reduction of silver are shown in Figure 5 for films with a thickness of 10 nm, 30 nm, and 50 nm. It is clear from these images that the reactivity is enhanced or suppressed differently in different domains and that it becomes less spatially selective with increasing film thickness. In fact, for the case of the 100 nm thick film in Figure 6, there is no obvious spatial selectivity. For each of the images in Figure 5, a line profile was taken from similar places on images before the reaction (not shown) and after the reaction; these are compared in Figure 5b, d, and f.

In Figure 5a, it is clear that silver has deposited in a striped pattern matching the pattern of 90° domain boundaries in $BaTiO_3$.[35] Between the stripes, there appears to be considerably less reaction product, which indicates that the dipolar field enhances the reaction in specific spatial locations. To illustrate the difference in reactivity between domains with enhanced and suppressed reactivity, height profiles perpendicular to the domains are plotted in Figure 5b. The height on top of the reactive domains is between 50 and 150 nm greater than the heights of the areas between reactive domains. The image of the surface of the 30 nm thick film is similar. However, the height differences between the preferred domains and the less reactive areas are smaller, as illustrated in Figure 5d. For the 50 nm thick film, there are still clearly preferred areas. In Figure 5e, the shapes of the boundaries between preferred and less reactive areas indicate that they correspond to 180° domain boundaries.[35] It has been noted that on the bare $BaTiO_3$ surface, the 180° domain boundaries have enhanced reactivity.[34] While a similar phenomenon is sometimes observed on the heterostructures, it can not explain the thick bands of reaction product in these images. Note that while some areas are preferred, silver is deposited on the entire surface. The height profile in Figure 5f shows smaller differences between the preferred and nonpreferred areas.

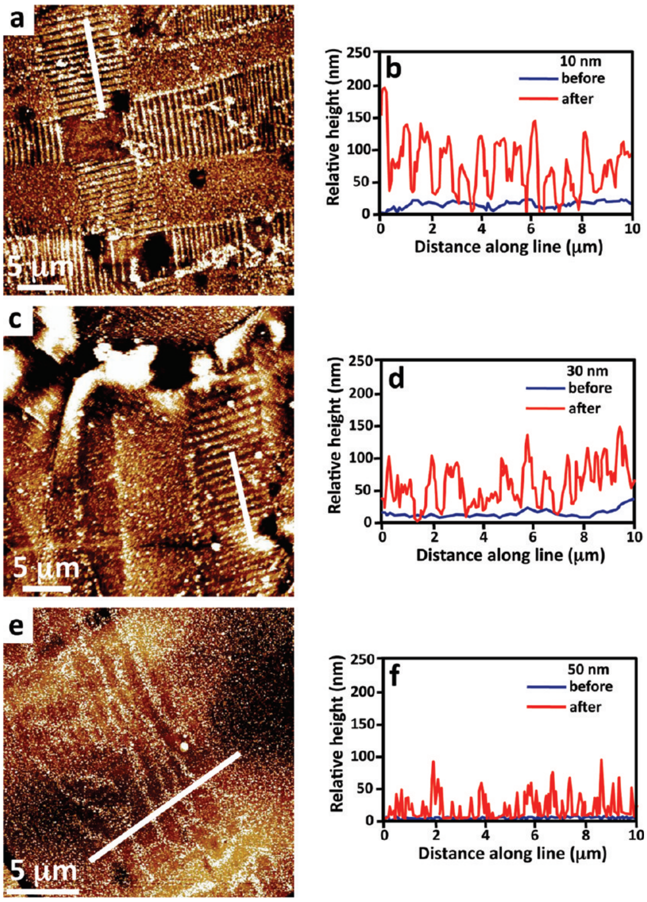

Figure 5. Topographic AFM images (a, c, and e) and height profiles (b, d, and f) for reacted TiO_2 films after silver reduction. Height profiles were extracted along the thick white lines. The before (blue) profiles were extracted from the same locations before the reaction. Panels a and b are for a 10 nm thick film; panels c and d are for a 30 nm thick film; and panels e and f are for a 50 nm thick film.

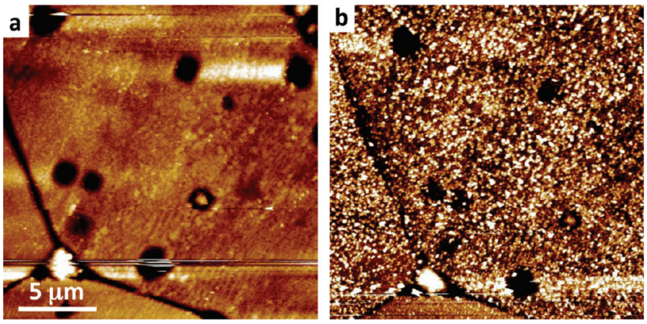

Figure 6. Topographic AFM images of 100 nm thick TiO_2 film surface (a) before reaction and (b) after reaction (silver nitrate, 15 s). Black-to-white contrast is 200 (a) and 175 nm (b).

One film was grown with a deliberately enhanced donor concentration. Unintentionally doped TiO_2 is an *n*-type

---

(35) Forsbergh, P. W., Jr. *Phys. Rev.* **1949**, *76*, 1187.

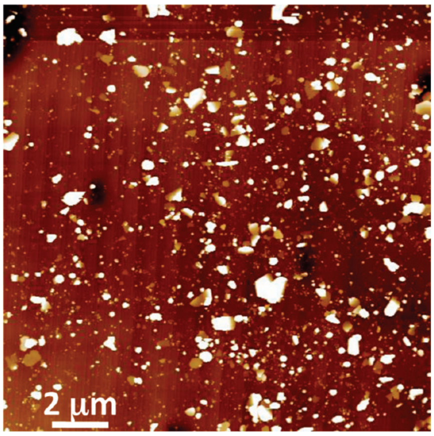

Figure 7. Topographic AFM images of a 15 nm thick Nb-doped TiO_2 film surface after reaction in silver nitrate solution. The film is (001) anatase on (100) $BaTiO_3$ and the black-to-white contrast is 80 nm.

semiconductor with a carrier concentration in the $10^{18}-10^{19}/cm^3$ range.[29] These carriers probably arise from oxygen vacancies. Based on the amount of Nb added to the film, the carrier concentration in the doped film is taken to be $3 \times 10^{20}/cm^3$. The surface of a 15 nm thick film of (001) anatase on (100) $BaTiO_3$ after the reduction reaction is shown in Figure 7. On this film, there is no indication of spatial selectivity. This result was also found on rutile films with (100) and (110) orientations. However, by surveying many areas, a few grains (with undetermined orientations) did show signs of weak spatial selectivity. So, while the spatial selectivity was quenched in most regions, it persisted in a minority of grains.

4. Discussion

Previous studies of the surface reactivity of ferroelectrics have led to the conclusion that for positive domains, in which the polarization is pointed toward the surface, the bands are bent downward (see Figure 8a), and this promotes the transfer of electrons to the surface and the reduction half reaction.[14−19] Oppositely oriented domains bend bands further upward (see Figure 8c), promoting the transfer of holes to the surface and oxidation reactions. In the work preceding this paper, this general line of reasoning was extended to interpret the reactivity of heterostructures.[22−25] If electrons accumulated at the surfaces of positive domains, then in the heterostruture electrons will accumulate at the internal $BaTiO_3/TiO_2$ interface. This implies that holes in the titania film should be repelled from the $BaTiO_3/TiO_2$ interface, promoting hole transfer and oxidation reactions on the TiO_2 surface. In other words, while the free surface of a positive $BaTiO_3$ domain promotes reduction, the surface of the same domain, when covered by a titania film, was assumed promote oxidation. The results presented here, particularly in Figure 3, indicate that this is not what happens. The reaction on the film surface is the same as the reaction promoted by the domain without a film.

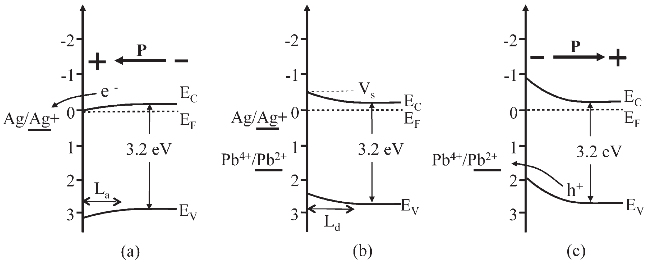

Figure 8. Schematic energy level diagrams for $BaTiO_3$ (a) for the case of a positive domain, (b) the case for nonpolar $BaTiO_3$ or titania, and (c) the case of a negative $BaTiO_3$ domain. The zero of the energy scale is the hydrogen reduction reaction.

This observation implies that the carriers that produce the patterns of reaction products on the surface are generated in the substrate and travel through the film to react on the surface. To understand this, we can consider the factors that influence the generation of charge carriers and their transport to the surface. The first factors that must be considered are the band gaps. $BaTiO_3$ is dichroic (the optical absorption is different in different directions), and it has also been noted that the optical absorption edge has a tail that makes it difficult to define an exact band gap.[36,37] For the simple models applied here, we assume a single band gap of 3.2 eV, which is within the range of observed values.[36,37] Titania is also dichroic and presents itself in two different phases (rutile and anatase) that have different bandgaps. On the basis of the available data, the room-temperature band gap of rutile can be taken to be 3.0 eV and the band gap of anatase can taken to be 3.2 eV.[29,38−40] Therefore, the bandgaps of the three materials differ by no more than 0.2 eV.

The absorption coefficients specify the amount of light absorbed in a certain thickness and, therefore, the concentration of photogenerated charge carriers that are produced. The emission spectrum of the Hg lamp used in the current experiment is structured and the most intense peak in the spectrum, at an energy greater than the band gap, is at 3.44 eV.[41] Therefore, we will take the absorption coefficients at this energy as representative values. Measured values indicate that rutile is much more strongly absorbing at this energy (1×10^5/cm)[40,42] than anatase (2×10^3/cm).[42,43] On the basis of these values, a 15 nm thick anatase (rutile) film absorbs on 0.3% (14%) of the incident photons and a 100 nm thick film absorbs 2% (67%) of the photons. The absorption coefficient of $BaTiO_3$ is similar to rutile, so the majority of the light should be absorbed in the space charge region of $BaTiO_3$. Therefore, for all but thick rutile films (no results from these films were presented in this paper), the substrate dominates the absorption and the majority of electron−hole pairs are generated there. Considering the fact that less than 14% of all carriers are generated in the film, it

---

(36) Wemple, S. H. *Phys. Rev. B* **1970**, *2*, 2679.
(37) Hafid, L.; Godefroy, G.; El Idrissi, A.; Michel-Calendini, F. *Solid State Commun.* **1988**, *66*, 841.
(38) Grant, F. A. *Rev. Mod. Phys.* **1959**, *31*, 646.
(39) Pascual, J.; Camassel, J.; Mathieu, H. *Phys. Rev. B* **1978**, *18*, 5606.
(40) Tang, H.; Levy, F.; Berger, H.; Schmid, P. E. *Phys. Rev. B* **1995**, *52*, 7771.
(41) http://www.newport.com/images/webclickthru-EN%5Cimages/1013.gif (accessed June 1, 2010).
(42) Park, Y. R.; Kim, K. J. *Thin Solid Films* **2005**, *484*, 34.
(43) Sekiya, T.; Ichimura, K.; Igarashi, M.; Kurita, S. *J. Phys. Chem. Solids* **2000**, *61*, 1237.

seems reasonable that most of the carriers that react on the surface are generated in the substrate. If it were the carriers generated in the film that dominated the reactions, we would expect reactivity to increase with film thickness (as more carriers are available) until the point where all the light is absorbed in the film and the substrate does not inflence the carriers. However, this is not consistent with the observations (see Figure 5). The results suggest that the carriers come from the substrate and that they travel across the internal $BaTiO_3 \| TiO_2$ interface to reach the surface.

The goal of the remainder of the discussion section is to develop a plausible energy level diagram for the heterostructure that can be used to understand the observations. It has already been mentioned that the band gaps are similar. According to measurements of the flat band potentials, the relative positions of the conduction band edges are also similar.[44,45] Kung et al.[44] reported that the flat band potential of rutile is about 0.05 V more positive than $BaTiO_3$ and Kavan et al.[45] reported that the flat band potential of anatase is 0.2 V more negative than rutile. So, these band edges are all within a 200 mV window. Furthermore, all three materials are *n*-type semiconductors, with a donor state about 0.2 eV below the conduction band edge; this would place the Fermi level about 0.1 eV below the conduction band edge.[29,46] The donor states in the film are associated with oxygen vacancies that are incorporated during the growth process. Because the growth temperature is more the 500 °C above the Curie temperature, there is no polarization and the vacancies will be distributed homogeneously and not contribute to the spatially localized reactivity.

Considering these similarities, a simple model is proposed based on the assumption that all of the materials have the same bandgap (3.2 eV), conduction band edge position, and Fermi level. This is obviously an approximation. In reality, the bands will have to shift by small amounts to account for differences in the absolute positions of these levels and there will be some charge transfer between the substrate and the film to account for differences in the Fermi level. Furthermore, these small shifts will be different for different orientations of the substrate and film (the effects of orientation and phase are described in the companion paper).[27] Because the available data indicate that these differences are all less than 200 mV, we will assume that the effects of band misalignment can be ignored. Note that using this approximation, the energy level diagram for bulk titania and a neutral $BaTiO_3$ domain are identical (see Figure 8b).

As a final consideration, the interaction of the surface with the solution also causes some band bending. Titania is weakly acidic and in aqueous solution is known to store negative charge on the surface in the form of hydroxyls. This leads to upward band bending. Morrison[47] notes that a good estimate for the surface potential (V_s) with respect to the Fermi level is simply the value of the flat band potential. When the value reported by Kung et al.[44] is adjusted to neutral pH, it is about $0.5V$, which was used to position V_s in Figure 9.

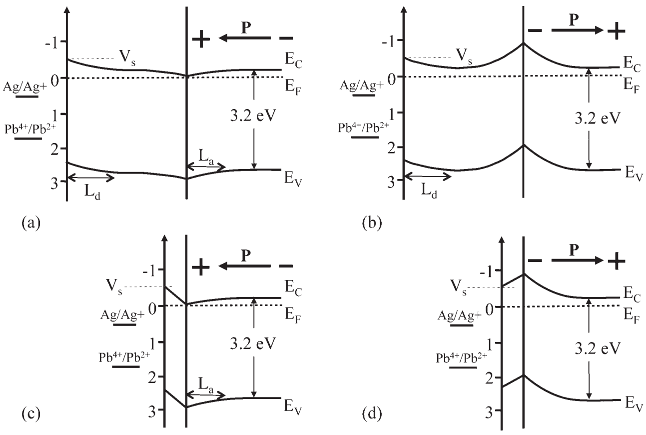

Figure 9. Schematic energy level diagrams for $TiO_2 \| BaTiO_3$ heterostructures for thick (a, b) and thin (c, d) films on positive (a, c) and negative (b, d) domains.

To generate plausible energy level diagrams for the heterostructures that can be used to interpret our results, the diagram for the film (Figure 8b) must be combined with those of the positive (Figure 8a) or negative domains (Figure 8c).[48−50] This is simple for the case of the films that are relatively thick (compared to the depletion width which is less than 100 nm). In these cases, illustrated in Figure 9a and b, the bands bend at the interface and at the surfaces, but return to the flat band condition between these limits. For the case of films that are thinner than the depletion width (see Figure 9c and d), the band positions are not able to fully relax.[51] If we assume that V_s is constant with film thickness (this amounts to assuming that the system can come to equilibrium with the solution at all thicknesses), and that the titania bands must meet the $BaTiO_3$ bands at the buried interface, then the energy level diagrams in Figure 9c and d result. The conduction and valence band level are drawn as straight lines. While there may be some curvature, it is likely small compared to the available thermal energy.

With reference to these energy level diagrams, we reconsider the observation that reactions on the 15 nm thick films occur in the same patterns as on the substrate, as if the film was not there. While the absorption coefficients and the experimental observations indicate that carriers come principally from the substrate, the schematic diagrams in Figure 9 indicate that there is a barrier for the transport of both carriers. The experiments, however, indicate that the barriers do not prevent reaction. This is not too surprising considering the fact that there is an approximately 0.5 eV barrier for the transport of electrons to the surface of bulk titania, yet it is still

---

(44) Kung, H. H.; Jarrett, H. S.; Sleight, A. W.; Ferretti, A. *J. Appl. Phys.* **1977**, *48*, 2463.
(45) Kavan, L.; Grätzel, M.; Gilbert, S. E.; Klemenz, C.; Scheel, H. J. *J. Am. Chem. Soc.* **1996**, *118*, 6716.
(46) Berglund, C. N.; Braun, H. J. *Phys. Rev.* **1967**, *164*, 790.
(47) Morrison, S. R. *Electrochemistry at Semiconductor and Oxidized Metal Electrodes*; Plenum Press: New York, 1980; p 137.
(48) Wurfel, P.; Batra, I. P. *Phys. Rev. B* **1973**, *8*, 5126.
(49) Watanabe, Y. *Solid State Ionics* **1998**, *108*, 59–65.
(50) Watanabe, Y. *Phys. Rev. B* **1998**, *59*, 11257.
(51) Albery, W. J.; Bartlett, P. N. *J. Electrochem. Soc.* **1984**, *131*, 315.

effective in photochemically reducing silver.[32,33] There are two factors that help carriers overcome this barrier. One is that photogenerated carriers produced during illumination will at least partially screen the charge at the interfaces and reduce the barrier for carriers to get to the surface.[18] It is also possible that the electrons (holes) that make it to the surface are in states above (below) the conduction (valence) band edge and are not stopped by the barrier, or that carriers driven to the internal interface tunnel through the film to react on the surface. Both of these mechanisms would imply that fewer carriers should make it to the film surface than on the bare substrate and that the heterostructures should be less reactive and the substrates. This is consistent with the experiment; to deposit similar amounts of silver or lead on the surface, the films must be reacted longer than the bare substrate.

As the films increase in thickness, the spatial selectivity diminishes until it disappears altogether. For the thin film heterostructure, the majority of the light is absorbed in the substrate so it is the band bending in the substrate that determines the reactivity. As a result, the energy level diagram in Figure 9d illustrates the situation that favors reduction. In the transition region, there is a mixture of carriers generated in the substrate and film. The carriers generated in the film probably account for the uniform component of the reactivity and the carriers from the substrate contribute to the spatially selective component. As the films become thicker, and a greater fraction of the carriers are generated further from the ferroelectric, the uniform component of the reactivity becomes larger and eventually dominates.

The Nb-doped samples have a higher carrier density than the undoped samples and the spatial selectivity is quenched for most grains. The dissolved Nb influences carrier density, optical absorption, and charge carrier scattering. First, it increases the density of carriers. This will lead to a decrease in the width of the space charge layer. Assuming that the bands in the film can relax toward bulk levels, this should reduce the barrier for charge to transfer from the substrate to the surface. However, this does not explain the absence of spatial selectivity. Another possibility is that donors in the film are able to screen the polarization in the $BaTiO_3$ and that this decreases the width of the space charge in the substrate. If so, fewer charges are separated and promoted toward the surface. Second, it is possible that Nb-doping causes more light to be absorbed in the film and less in the substrate. However, doping of this type is more likely to affect the tail of the absorption peak than the band edge. A third possibility is that the dissolved Nb increases the rate of ionized donor scattering and recombination.[52,53] Scattering may change the direction of the carriers and reduce the reactivity, leading to the absence of spatial selectivity and lower reactivity of the surface. Finally, it should also be noted that if a substantial amount of Nb diffused into the substrate during growth, this would also reduce polarization and spatial selectivity.

The details of the interface and how it influences the reactivity of the films are still in question, but on the basis of the current observations, it seems clear that it is the carriers in the substrate that react on the surface. This interpretation is consistent with the observations of the reactivity of titania films on $LiNbO_3$.[23] Inoue et al.[23] used light with a lower energy than the substrate's band gap and could be sure that all of the carriers were generated in the film. In this case, the film reactivity increased with film thickness until a maximum at about 100 nm. The fact that the substrate contributes to the surface reactivity of the thin films in the present experiments suggests that the substrate can serve as a source of charge carriers and is important in the design of composite photocatalysts using ferroelectric components.

5. Conclusion

Titania films grown on $BaTiO_3$ substrates, when illuminated by UV light, photochemically reduce Ag^+ to Ag^0 and oxidize of Pb^{2+} to Pb^{4+} in patterns determined by the domain structure of the substrate. The results indicate that dipolar fields from the ferroelectric domains cause carriers generated in the substrate to travel through the film to react on the film surface just as they would on the substrate surface. The influence of the ferroelectric substrate on the pattern of reactants is diminished as the film thickness increases and a greater fraction of the light is absorbed in the film. The spatial selectivity of the reaction is also quenched when the film is donor-doped with Nb.

Acknowledgment. The work was supported by National Science foundation grants DMR 0412886 and DMR 0804770.

---

(52) Emeline, A. V.; Furubayashi, Y.; Zhang, X.; Jin, M.; Murakami, T.; Fujishima, A. *J. Phys. Chem. B* **2005**, *109*, 24441.

(53) Miyagi, T.; Kamei, M.; Sakaguchi, I.; Mitsuhashi, T.; Yamazaki, A. *Jpn. J. App. Phys.* **2004**, *43*, 775.